

SPATIAL RESOLUTION REQUIREMENTS FOR
NUMERICAL SIMULATION OF INTERNALLY
HEATED FLUID LAYERS

Günther Grätzbach

Kernforschungszentrum Karlsruhe
Institut für Reaktorentwicklung
7500 Karlsruhe, Fed. Rep. Germany

ABSTRACT

Direct numerical simulations are performed for turbulent convection in an infinite horizontal fluid layer. At a Rayleigh number of 4×10^6 grids with 16^3 to 64^3 nodes are used to test criteria for the spatial resolution capabilities of grids. It is seen that Nusselt numbers and other statistical quantities are insensitive to the number of nodes, whereas energy spectra and flow patterns are rather critical results. These demand about 32^3 nodes in minimum for sufficient accuracy. This value is also predicted by calculating the coefficient of a subgrid scale heat flux model.

1 INTRODUCTION

For the detailed numerical description of turbulent heat transport in volumetrically heated fluid layers direct numerical simulation and statistical turbulence models are preferably used. The statistical models as in [1,2] are based on time averaged conservation equations. Therefore, models have to be introduced which must represent the total information about turbulence. The direct methods are based on the complete, non-steady, three-dimensional conservation equations. Only when coarse grids are used, subgrid scale models are necessary for the unresolved turbulence elements. In general the direct method is not fully implemented for this type of flow: The papers [2-5], e.g., are based on two-dimensional basic equations. As compared to statistical models higher universality and real 'prediction' capabilities

Conf. on Numerical Methods in Laminar and Turbulent Flow. □

Venice, Italy, July 13 - 16, 1981, □

in: "Numerical Methods in Laminar and Turbulent Flow", □

Taylor, C., Schrefler, B. A., Ed., p. 593-604, Pineridge Press Ltd. (1981) □

As boundary conditions for an infinite plane channel periodicity is assumed in both horizontal directions with periodicity lengths X_1 and X_2 . In the vertical direction the velocities are set to zero at the walls, and the wall shear stresses and wall heat fluxes are approximated by linear finite differences using the velocities and temperatures in the wall adjacent grid cells.

Equations (1) already contain turbulence assumptions. The unknown averaged convective terms are split in a large scale part \bar{y} and in a subgrid scale part y' ,

$$\overline{u_i u_j} = \overline{u_i} \overline{u_j} + \overline{u_i' u_j'} \quad (2a)$$

$$\overline{u_j T} = \overline{u_j} \overline{T} + \overline{u_j' T'} \quad (2b)$$

and the subgrid scale terms are neglected. To justify this neglect it has to be investigated by use of calculated Nusselt numbers, energy spectra and vortex patterns, e.g., whether the grid widths chosen are small enough to resolve the smallest relevant turbulence elements.

3 SPATIAL RESOLUTION REQUIREMENTS

The most important requirements for spatial resolution of grids used in direct numerical simulations are prescribed by the main features of laminar and turbulent convection:

1. The flow patterns in channels with large horizontal extensions consist of large scale vortex systems with maximum wavelengths of typically some channel heights $\bar{L}_{9,10,11}$. The periodicity lengths X_1 should be chosen large enough to capture these large scale structures. Comprehensive data on the maximum wavelengths observed are not known. Thus, X_1 must be determined by numerical tests.

2. In addition, the convection patterns contain very small scale structures. The horizontal extension of the observed cold blobs falling from the upper wall to the channel center, e.g., is about one order of magnitude smaller than the channel height \bar{L}_{10} . Again, the grid widths necessary to resolve these small scale structures have to be determined by numerical tests.

3. Most statistical flow data in channel flows show strong space dependence near the walls, like the steep temperature gradients in the thermal boundary layer δ , and the sharp maximum values of velocity and temperature fluctuations, and the turbulent heat flux in the transition layer to the isothermal turbulent core. A recommendation for the vertical grid width distribution can be deduced from experimentally deduced temperature profiles $\bar{L}_{9/}$ and from numerical experience $\bar{L}_{12/}$: It seems sufficient to have three to four nodes within the thermal boundary layer,

would be the advantages of direct methods using the complete conservation equations $\bar{L}_{6/}$.

In this paper the computer code TURBIT-3 $\bar{L}_{7/}$ is used for direct numerical simulation of turbulent convection. This code is based on a finite difference form of the complete conservation equations for mass, momentum and heat. To justify the neglect of subgrid scale models, the most important spatial resolution requirements for grids are investigated by numerical simulations with different grids at a fixed Rayleigh number of $Ra = g\beta_0 D^5 / (\nu\alpha K) = 4 \times 10^6$, with $\dot{q} =$ volumetric heat source, $D =$ channel height, $\alpha =$ thermal diffusivity. A theoretical way to test grids in advance of applications is also applied.

2 NUMERICAL SIMULATION MODEL

The simulation model TURBIT-3 is based on the complete, three-dimensional, non-stationary conservation equations for mass, momentum and heat. Constant material properties and the validity of the Boussinesq approximation are assumed. Cartesian coordinates are used with x_1 and x_2 horizontal and x_3 directed upwards.

To get a finite difference scheme these equations are integrated formally over the mesh volume $V = \Delta x_1 \Delta x_2 \Delta x_3$. Application of the Gaussian theorem to the volume average of partial derivatives directly gives a finite difference form $\delta_i \bar{y}$ for surface average values \bar{y} , where y is any variable and i is the direction normal to the mesh cell surface. A staggered grid is used to get exact mass conservation, but this does not eliminate the need for some linear averages \bar{y} to approximate variables between two nodes. As deduced in $\bar{L}_{8/}$, this results in the following explicit finite difference scheme, in which the space averaging bars have been omitted, the summation convention is used for repeated lower indices, and the superscript n refers to the time step $t^n = n \Delta t$:

$$(\bar{u}_i^{n+1} - \bar{u}_i^{n-1}) / (2 \Delta t) = - \delta_j (\bar{u}_j^j \bar{u}_i^j)^n + \delta_j (\nu \delta_j \bar{u}_i)^{n-1} \quad (1a)$$

$$- g\beta_0 (T_{ref} - T)^n$$

$$\frac{1}{\rho} \delta_i \delta_i \bar{p}^n = \delta_i \bar{u}_i^{n+1} / (2 \Delta t) \quad (1b)$$

$$i = 1, 2, 3$$

$$\bar{u}_i^{n+1} = \bar{u}_i^{n-1} - 2 \Delta t / \rho \delta_i \bar{p}^n \quad (1c)$$

$$(\bar{T}^{n+1} - \bar{T}^{n-1}) / (2 \Delta t) = - \delta_j (\bar{u}_j \bar{T}^j)^n + \delta_j (\alpha \delta_j \bar{T})^{n-1} + \dot{q} / (\rho C_D) \quad (1d)$$

and about the same number in the transition layer $\delta < x_3 < 2.5 \delta$. The layer thickness $\delta/D = 1/Nu$ can be evaluated from known Nusselt number correlations [9,10,13] in advance of simulations.

In case of limited computing time and storage capabilities, criterion 2 may be replaced by use of subgrid scale models, and criterion 3 by use of universal profiles to approximate the wall conditions. This is the approach chosen for the simulation of high Reynolds number forced convection [7,6].

4 NUMERICAL SEARCH FOR REQUIRED GRID WIDTHS

4.1 Initial Conditions

Four simulations with different grids have been performed for a Prandtl number of $Pr = 6$ and for a Rayleigh number of $Ra = 4 \times 10^6$ (Table 1). The horizontal node numbers N_1 and N_2 and the respective grid widths Δx_1 and Δx_2 have been varied together to get fixed periodicity lengths $X_1 = N_1 \Delta x_1 = 2.8$. This value has been used for simulations of Bénard convection [12,14]. The vertical grid widths near the lower and upper wall, Δx_{3w1} and Δx_{3w2} , agree for all cases with criterion 3.

Case	$N_1=N_2$	N_3	$\Delta x_1=\Delta x_2$	Δx_{3w1}	Δx_{3w2}	Δx_{3mex}	t_{max}	NT	CPU-time min/IBM
5	16	16	.175	.044	.027	.158	143.1	4120	127.5/168
7	32	16	.0875	.044	.027	.158	168.9	7880	542.7/3033
10	32	32	.0875	.0325	.020	.0325	123.6	9600	1358.1/3033
11	64	32	.04375	.0325	.020	.0325	40.2	4040	2293.4/3033

Table 1: Case specifications and time intervals. t_{max} = time interval simulated, NT = number of time steps.

The three dimensional velocity fields at time $t=0$ have been set to zero. The initial temperature fields were generated to have an isothermal mean temperature (average over horizontal planes) in the turbulent core and a linear decrease within the thermal boundary layers to the constant wall temperatures $T_w1 = T_w2$. To this trapezoidal profile random fluctuations have been superposed with a maximum amplitude of 25 % of the time mean temperature difference $\Delta T_c = \langle T_{max} - T_w \rangle$. This type of initial conditions reduces the computing times necessary to approach fully developed flow and makes the computed statistical data independent of initial conditions [12].

An approximate universal presentation of numerical results is forced by normalizing Eq. (1) with a length D , a time $D^2 / (\nu_0)$, a velocity $\sqrt{g\beta\Delta T_0 D}$, and a temperature ΔT_0 . The latter is calculated using a dependence between the Camköhler and Nusselt numbers: $De = \dot{Q} D^2 / (K \Delta T_0) = Nu_1 + Nu_2$. Application of the correlations in [13] results in $Da(t=0) = 15.72$.

4.2 Examination of Numerical Results

Equations (1) are integrated in time until steady-state conditions, in a statistical sense, are established for a period suitable for evaluation. The respective problem times and numbers of time steps are indicated in Table 1. To get reasonable statistical data from the non-steady numerical results, averages $\langle y \rangle$ are formed over horizontal planes and over 15 to 60 arbitrary time steps.

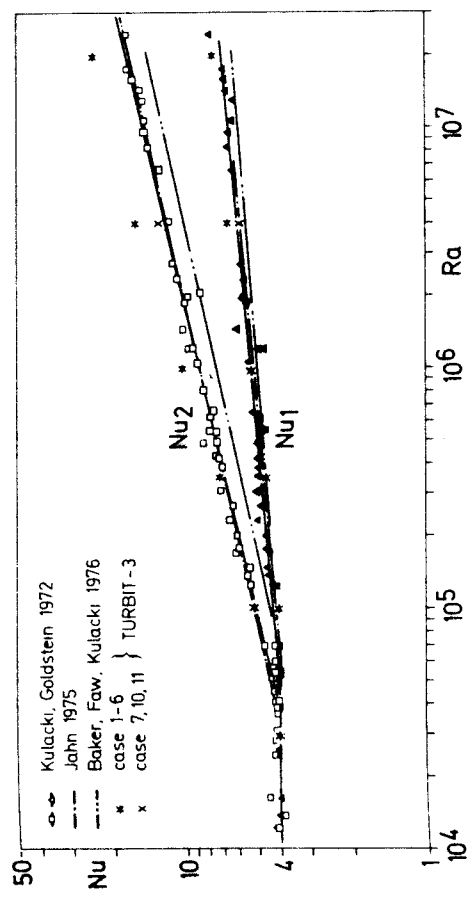


Fig. 1: Rayleigh dependence of the Nusselt numbers

The Nusselt numbers calculated for both walls are compared to experimental data in Fig. 1. The figure contains further results for different Rayleigh numbers but equal grids. The numerical results for small Ra agree with experimental data. With increasing Ra the experimental data are overestimated. Only cases 7, 10 and 11 are within the scatter-band of experimental data. The decrease in Nu_1 from case 5 to 7 is obtained for constant vertical grid widths changing the horizontal ones (Table 1). Thus the region near the wall (criterion 3) seems to be resolved adequately by grid 5, but not the turbulent core.

Most sensitive indicators for insufficient spatial resolution are calculated energy spectra of velocity fluctuations (Fig. 3). Two spectra of case 5 are completely non-physical, because the energy does not decrease at high wave numbers $K_1 = \pi/(m \Delta x_1)$, with $1 \leq m \leq N_3/2$. Comparison to case 11 shows that grid 5 neglects about 1% of energy of the horizontal fluctuations, and less than 10% of the most important vertical fluctuations. Of course, these fractions would be much larger in terms of vorticity spectra, and so grid 5 is the only one which definitely calls for a subgrid scale model to represent the damping caused by the small vortices containing this energy.

Contour line plots of temperature fields for case 5 at $t=127$. The contour line increment Δ is .0625 for the vertical section, and .025 for the horizontal section. Origins of sections are denoted by additional arrows.

A 1% limit has also been found with direct simulations of Bénard convection [14].

Contour line plots of instantaneous temperature fields are given in Figs. 4 to 6 and are compared to experimental results [10]. In the vertical sections the cold blobs falling from the narrow cold upper thermal boundary layer into the nearly isothermal hot core of the channel are recorded appropriately by grid 11 (Fig. 5) and are in qualitative agreement with the interference pictures from [10], but are insufficiently recorded by grid 5 (Fig. 4).

The reason why the horizontal grid widths have the largest influence on statistical data becomes evident from the horizontal sections through the upper half of the channel: Very narrow spoke-pattern like structures are formed in

The maximum values of the vertical root mean square velocity and temperature fluctuation profiles are shown in Fig. 2 as a function of the reciprocal mean grid width $\bar{n} = (\Delta x_1 \Delta x_2 \Delta x_3)^{1/3}$, with $\Delta x_3 = 1/N_3$. The results are normalized by ΔT calculated to eliminate its deviation from ΔT_0 . As expected, the local statistical data on turbulent fluctuations are more sensitive to the grid widths than the Nusselt numbers. The slight decrease of the rms values from grid 7 and 10 to 11 is within the statistical uncertainty of $\pm 5\%$ of these results.

Fig. 2: Dependence of the maximum rms values on the mean grid width

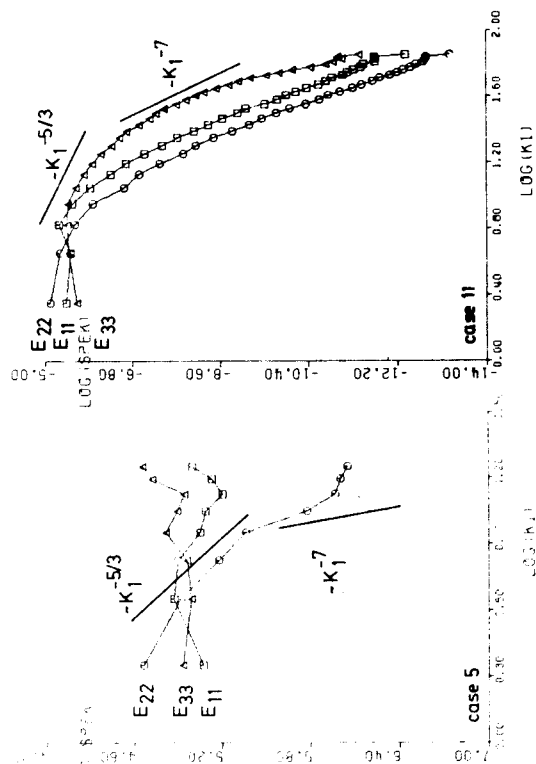
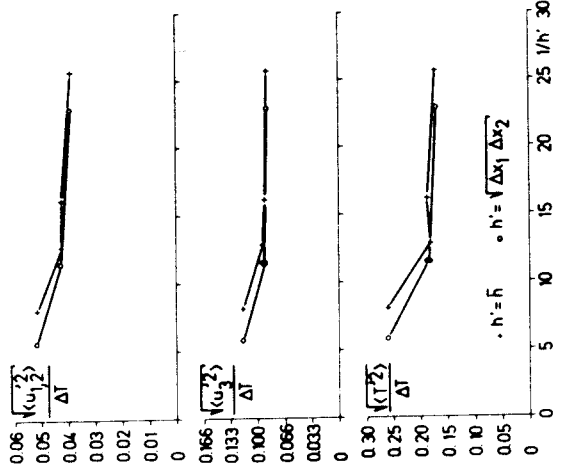


Fig. 3: Energy spectra for the velocity fluctuations $\langle u_i^2 \rangle = \langle u_i u_i \rangle - \langle u_i \rangle^2$, calculated from space dependent results at $x_3 = 0.89$

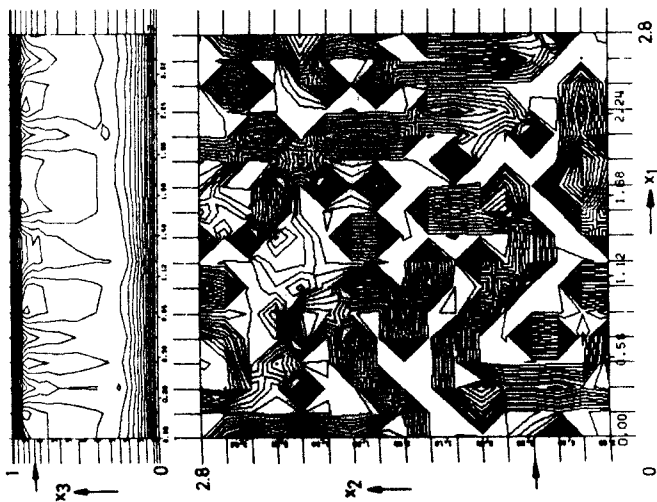


Fig. 4: Contour line plots of temperature fields for case 5 at $t=127$. The contour line increment Δ is .0625 for the vertical section, and .025 for the horizontal section. Origins of sections are denoted by additional arrows.

A 1% limit has also been found with direct simulations of Bénard convection [14].

Contour line plots of instantaneous temperature fields are given in Figs. 4 to 6 and are compared to experimental results [10]. In the vertical sections the cold blobs falling from the narrow cold upper thermal boundary layer into the nearly isothermal hot core of the channel are recorded appropriately by grid 11 (Fig. 5) and are in qualitative agreement with the interference pictures from [10], but are insufficiently recorded by grid 5 (Fig. 4).

The reason why the horizontal grid widths have the largest influence on statistical data becomes evident from the horizontal sections through the upper half of the channel: Very narrow spoke-pattern like structures are formed in

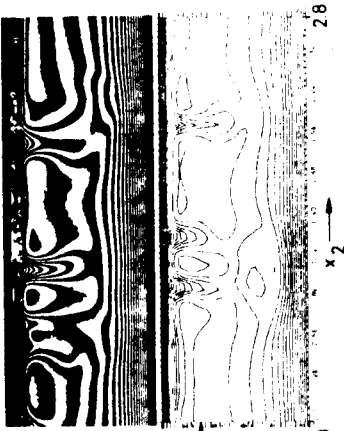


Fig. 5: Vertical temperature field for $Ra = 3.7 \times 10^6$ / 10 and below for case 11 at $t = 31$. $\Delta = .0625$. The arrow denotes the origin of Fig. 6.

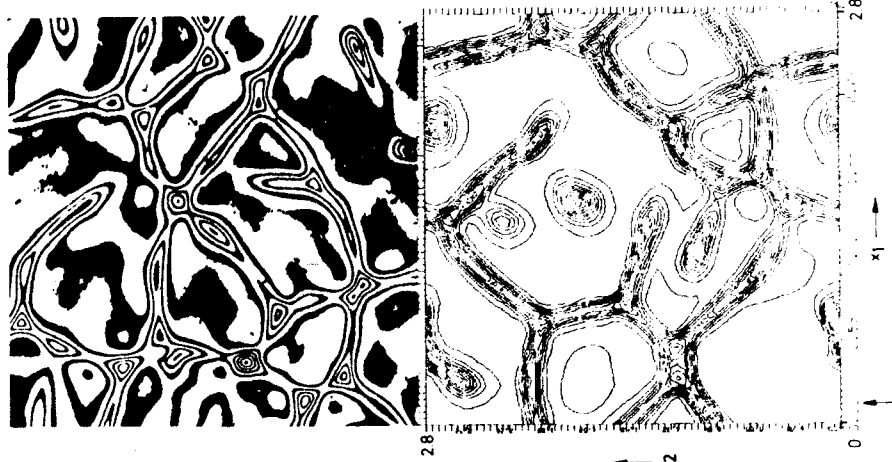


Fig. 6: Horizontal temperature fields deduced experimentally / 10 and below for case 11. $\Delta = .0625$. The arrow denotes the origin of Fig. 5

experiment / 10 and also in high resolution numerical studies like in case 11 (Fig. 6). Such structures are totally absent in the horizontal section for case 5 (Fig. 4). Thus, the spatial resolution of case 5 is far from being sufficient.

5 THEORETICAL INVESTIGATION OF THE REQUIRED GRID WIDTHS

The subgrid scale heat flux model implemented in the TURBIT-code has successfully been used to judge on the spatial resolution capabilities of grids for Bénard convection / 14 and for forced liquid metal flows / 15. Therefore, this model is applied here to the internally heated fluid flow problem.

The subgrid scale heat flux is proportional to a coefficient C_{T2} / 15. Assuming local isotropy for subgrid scale turbulence, this coefficient can be calculated on the basis of the Kolmogorov and Batchelor energy spectra for turbulent velocity and temperature fluctuations. For the constants in the spectra $\alpha = 1.5$ and $\beta = 1.3$ are used. This procedure gives:

$$C_{T2} = \frac{1 - \beta f_1(\Delta x_1)(Re_0 Pr)^{-1} V^{-4/9} \langle \epsilon \rangle^{-1/3}}{\beta \alpha^{1/2} f_2(\Delta x_1)} \quad (3)$$

The functions $f_j(\Delta x_1)$, which are of order one and which depend only on grid parameters, are irrelevant here. The second term of the numerator only is important for small mesh volumes or for small Reynolds numbers $Re_0 = u_0 D/\nu$, where $u_0 = \sqrt{g\beta \Delta T_0 D}$. For these limits an approximation for the dissipation $\langle \epsilon \rangle$ of turbulence energy has to be introduced to determine C_{T2} .

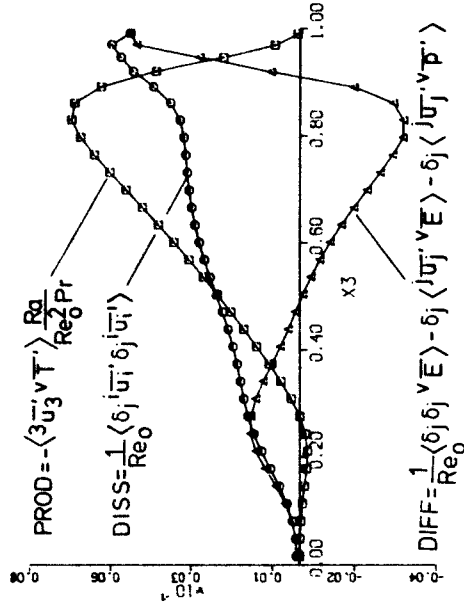


Fig. 7: Vertical profiles of terms of the conservation equation for the resolved turbulence energy $\overline{v \epsilon} = \langle \overline{u_i^2} \rangle / 2$

The dissipation, calculated from the results of case 11 (Fig. 7), is nonzero in the convection controlled lower area, where in accordance with estimations in / 16 a small

negative production is predicted. The nonzero dissipation is caused by the diffusion term which removes energy from the upper half to the lower half of the channel. For a rough estimate, the resulting smooth dissipation profile is approximated by a linear increase between the wall values $\langle \epsilon_{w1} \rangle = C$ and $\langle \epsilon_{w2} \rangle = (Nu_2 - Nu_1) Ra / (Re_0^3 Pr^2) / D_n$.

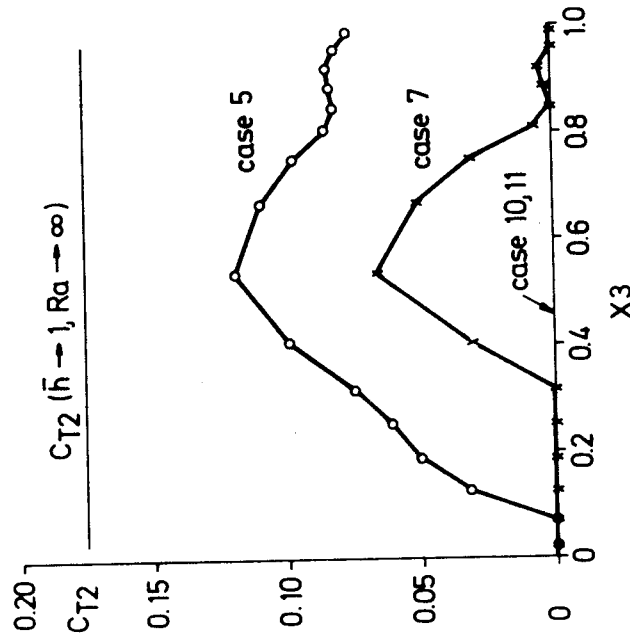


Fig. 8: Vertical profiles for the calculated coefficient C_{T2}

This approximation together with the complete theory indicated in Eq. (3) gives the results for C_{T2} shown in Fig. 8. The largest values appear for case 5; smaller ones for case 7; for case 10 and 11 the calculated values are zero. As the subgrid scale heat flux is proportional to C_{T2} , a subgrid scale model is necessary for cases 5 and 7, whereas practically all small scale turbulence elements are resolved in cases 10 and 11.

6 CONCLUSIONS

The Nusselt numbers calculated are slightly too high. This may indicate insufficient resolution of large vortices caused by too small periodicity lengths, because for the similar Bénard convection an increase in turbulent heat flux for decreasing wavelenghts is known [12]. Nusselt numbers and other statistical data are not very sensitive to insufficient resolution of small vortices. Sensitive results are energy

spectra and contour line plots. These are completely nonphysical in case 5, although all computed statistical data deviate by not more than 25 % from those of the other cases. The sharp requirements to the horizontal grid widths are due to the existence of flow structures with very small horizontal extensions.

Compared to Bénard simulation requirements [12,14,7], finer grids have to be chosen here despite lower degrees of turbulence, and other quantities are the real indicators for insufficient resolution. Thus, the indicators and the required grid widths depend strongly on the type of flow. For all flow types cited in this paper the statistical data usually considered are insensitive to insufficient subgrid scale modelling or insufficient spatial resolution. Thus, coarse grid simulations have to be carefully checked. The theory to calculate the coefficient of a subgrid scale heat flux model turned out to be a useful tool to predetermine grids with sufficient spatial resolution.

7 ACKNOWLEDGEMENTS

The author wishes to appreciate the lively discussions and many useful comments given to him by Dr. Ch. Homann and Dr. U. Schumann, Institut für Reaktorentwicklung, during the preparation of this paper. The careful typing by Mrs. H. Jansky is also kindly acknowledged.

8 REFERENCES

- 1 MAYINGER, F., JAHN, M., REINECKE, H.H., STEINBERNER, U. - Untersuchung thermohydraulischer Vorgänge sowie Wärmeaustausch in der Kernschmelze. Abschlußbericht BMFT-RS 46/1, Teil I, 1975
- 2 BIASI, L., CASTELLANO, L., HOLTBECKER, H. - Molten pool theoretical studies. PAHR-Information Exchange, ANL-78-10, Argonne, November 2-4, 1977
- 3 PECKOVER, R.S., HUTCHINSON, I.H. - Convective rolls driven by internal heat sources. Physics of Fluids, Vol. 17, pp. 1369-1371, 1974
- 4 REINECKE, H.H. - Numerische Berechnung der thermohydraulischen Vorgänge in einer Kernschmelze. Diss., Tech. University Hannover, 1974
- 5 EMARA, A.A., KULACKI, F.A. - Studies of heat source driven natural convection: A numerical investigation. RF 3746, Ohio State University

- 6 SAFFMAN, P.G. - Problems and progress in the theory of turbulence. Structure and Mechanisms of Turbulence II, Ed. H. Fiedler, Lecture Notes in Physics, Vol. 76, Springer-Verlag Berlin, 1978
- 7 GRÖTZBACH, G. - Numerical investigation of radial mixing capabilities in strongly buoyancy-influenced vertical, turbulent channel flows. Nuclear Engineering and Design, Vol. 54, pp. 49-66, 1979
- 8 SCHUMANN, U., GRÖTZBACH, G., KLEISER, L. - Direct numerical simulation of turbulence. Prediction Methods for Turbulent Flows, Ed. W. Kollmann, Hemisphere Publ. Corp., pp. 123-258, 1980
- 9 KULACKI, F.A., GOLDSTEIN, R.J. - Thermal convection in a horizontal fluid layer with uniform volumetric energy sources. J. Fluid Mech., Vol. 55, pp. 271-287, 1972
- 10 JAHN, M. - Holographische Untersuchung der freien Konvektion in einer Kernschmelze. Diss., Techn. University Hannover, 1975
- 11 IVEITEREID, M. - Thermal convection in a horizontal fluid layer with internal heat sources. Int. J. Heat Mass Transfer, Vol. 21, pp. 335-339, 1978
- 12 GRÖTZBACH, G. - Direct numerical simulation of laminar and turbulent Bénard convection. To appear in J. Fluid Mech.
- 13 BAKER Jr., L., FAW, R.E., KULACKI, F.A. - Post-accident heat removal I: Heat transfer within an internally heated nonboiling liquid layer. Nucl. Science Engng., Vol. 61, pp. 222-230, 1976
- 14 GRÖTZBACH, G. - Über das räumliche Auflösungsvermögen numerischer Simulationen von turbulenter Bénard-Konvektion. KfK 2981 B, Kernforschungszentrum Karlsruhe, 1980
- 15 GRÖTZBACH, G. - Numerical simulation of turbulent temperature fluctuations in liquid metals. To appear in Int. J. Heat Mass Transfer, 1981
- 16 KULACKI, F.A., GOLDSTEIN, R.J. - Eddy heat transport in thermal convection with volumetric energy sources. Fifth Int. Heat Transfer Conf., Tokyo, Vol. 3, pp. 64-68, 1974.

Numerical Methods in Laminar and Turbulent Flow

Editors:

C. Taylor

B. A. Schrefler

*Proceedings of the Second International
Conference held at Venice,
13th - 16th July, 1981*

PINERIDGE PRESS
Swansea, U.K.

First Published, 1981 by
Pineridge Press Limited
91, West Cross Lane, West Cross, Swansea, U.K.

ISBN 0-906674-15-8

Copyright © 1981 by Pineridge Press Limited.

British Library Cataloguing in Publication Data

Numerical methods in laminar and turbulent flow

1. Fluid dynamics - Mathematics - Congresses

I. Taylor, C. II. Schrefler, B.

532'.051015/117 QA911

ISBN 0-906674-15-8

Printed and bound in Great Britain by
Robert MacLehose and Co. Ltd.
Printers to the University of Glasgow